Msx1-Deficient Mice Fail to Form Prosomere 1 Derivatives, Subcommissural Organ, and Posterior Commissure and Develop Hydrocephalus

P. FERNÁNDEZ-LLEBREZ, PHD, J. M. GRONDONA, PHD, J. PÉREZ, PHD, M. F. LÓPEZ-ARANDA, G. ESTIVILL-TORRÚS, PHD, P. F. LLEBREZ-ZAYAS, E. SORIANO, PHD, C. RAMOS, PHD, Y. LALLEMAND, MD, A. BACH, AND B. ROBERT, MD

From the Departamento de Biología Celular, Genética y Fisiología, Facultad de Ciencias, Universidad de Málaga (PF-LL, JP, JMG, FLA), Málaga, Spain; Fundación para la Investigación Hospital Carlos Haya, Hospital Universitario Carlos Haya (GET, PFLL-Z), Málaga, Spain; Departamento de Biología Celular, Universidad de Barcelona (ES, CR), Barcelona, Spain; and Unité de Génétique Moléculaire de la Morphogenèse, Institut Pasteur, URA 1947 du CNRS (YL, AB, BR), Paris, France.

Correspondence to: P. Fernández-Llebrez, Departamento de Biología Celular, Genética y Fisiología, Facultad de Ciencias, Universidad de Málaga, Málaga E-29071, Spain. E-mail: llebrez@uma.es

Supported by DGICYT (BFI 2000-1360; BFI 2003-03348, Spain), FIS (01-0948; PIO2-1517, Spain), Red CIEN (Fundacio´n Hospital Carlos Haya; ISCIII, Spain) and by the Institut Pasteur, the CNRS, and grants from the Association pour la Recherche sur le Cancer and the Association Française contre les Myopathies.

Abstract.
Msx1 is a regulatory gene involved in epithelio-mesenchymal interactions in limb formation and organogenesis. In the embryonic CNS, the Msx1 gene is expressed along the dorsal midline. Msx1 mutant mice have been obtained by insertion of the nlacZ gene in the Msx1 homeodomain. The most important features of homozygous mutants that we observed were the absence or malformation of the posterior commissure (PC) and of the subcommissural organ (SCO), the collapse of the cerebral aqueduct, and the development of hydrocephalus. Heterozygous mutants developed abnormal PC and reduced SCO, as revealed by specific antibodies against SCO secretory glycoproteins. About one third of the heterozygous mutants also showed hydrocephalus. Other defects displayed by homozygous mutants were ependymal denudation, subventricular cavitations and edema, and underdevelopment of the pineal gland and subfornical organ. Some homozygous mutants developed both SCO and PC, probably as a consequence of genetic redundancy with Msx2. However, these mutants did not show SCOimmunoreactive glycoproteins and displayed obstructive hydrocephalus. This suggests that Msx1 is necessary for the synthesis of SCO glycoproteins, which would then be required for the maintenance of an open aqueduct.

Key Words: Circumventricular organs; CNS development; Diencephalic development; Immunocytochemistry; Mutant; Regulatory
genes; Transcriptional factors.

INTRODUCTION

The development of the vertebrate forebrain depends on the temporal-spatial expression of regulatory genes that establish a series of rostro-caudal subdivisions called prosomeres (1). The posterior commissure (PC) forms in the dorsal midline of prosomere 1 (P1). Beneath it the dorsal midline ependyma differentiates into a secretory circumventricular organ named the subcommissural organ (SCO), whose cells develop basal processes that intermingle with the PC fibers (2). The SCO secretes high molecular weight glycoproteins into the third ventricle that polymerize in a thick fiber known as Reissner's fiber (3). This fiber runs along the aqueduct, the fourth ventricle, and the spinal central canal and its function remains enigmatic. Polyclonal and monoclonal antibodies have been raised against SCO secretory glycoproteins (4, 5). These antibodies show that, in most vertebrates, the SCO begins its secretory activity at early developmental stages and is active for lifetime. In the chick and the duck, the secretory activity of the SCO precedes the appearance of axonal bundles in the PC (6). In contrast, the first immunocytochemical evidence for glycoprotein release in the rat was observed at E15 when a growing PC is still present (7). In the mouse, the SCO starts synthesizing glycoproteins at about E14.5 (8), while axonal bundles of the PC are visible beginning at E10.5 (9). The tight morphological relationship between the SCO cells and the PC, and the fact that SCO secretory glycoproteins stimulate in vitro neuronal adhesion and neurite extension (10), suggested some functional or developmental relation similar to that described for the spinal floor plate and the ventral commissure (11–13). Indeed, an SCO secretory glycoprotein was found to share homology with Fspondin and hence was called SCO-spondin. It is a candidate to exert axonal guidance properties (14, 15).

A developmental morpho-functional relationship between the SCO and the PC was also evident in mouse strains carrying mutations in certain regulatory genes. *Pax6* is an important gene for P1 development. Estivill-Torru´s et al demonstrated that *small eye* mutant mice that express a non-functional form of Pax6 protein fail to develop the SCO, the PC, and the pineal gland (8). Conversely, mutations in *Pax2/5* genes, which are expressed in the mesencephalon, led to the posterior extension of Pax6 expression domain, and correlatively, to the development of a caudally expanded PC over a thick subjacent ependyma morphologically similar to the SCO (16). Moreover, *Pax6* null mice mutants expressing *Pax6* under the control of *Pax2* enhancer sequences, although lacking a pretectum, developed an ectopic PC in the rostral-most mesencephalon, suggesting that expression of *Pax6* in a population of responsive cells in the caudal diencephalon induces PC formation (16). On the other hand, ectopic expression of *En1* in the territory of *Wnt1*, including the dorsal midline of P1, led to the absence of formation of the SCO and severe errors in axonal pathfinding of the PC (17). Thus, there seems to be a functional link between the development of SCO and of the PC.

A common feature in animal models lacking SCO, or with abnormal SCO, is the development of hydrocephalus. This pathology is observed in *Pax6* (18) and *Wnt1* mutants, correlatively with an alteration in SCO formation (17, 19). Mutants for the *Msi1* gene, which encodes an RNA-binding protein of the Musashi family, also show malformations in the SCO and the aqueduct and obstructive hydrocephalus (20). Also, mutants for the transcription factor RFX4pv3 fail to develop SCO and showed

hydrocephalus (55). Hydrocephalus was also observed in several rodent spontaneous mutants showing deficient development of the SCO (21–27), as well as in humans (28). Hydrocephalus has further been related to abnormal development of the SCO after experimental manipulations such as X-irradiation (29) or folic acid and/or vitamin B12 deficiency during development (30, 31). These authors suggested that the secretory activity of the SCO is responsible for the maintenance of an open aqueductal cavity. Indeed, it has been shown that immunological blockade of SCO in developing rats by immunizing pregnant rats with RF glycoproteins led to dysfunctions in SCO, aqueductal stenosis, and hydrocephalus (32). Thus, it seems that a healthy SCO is a requirement for a normal cerebrospinal fluid circulation.

Msx genes encode homeodomain transcription factors that are expressed dorsally in the neural tube of all species throughout chordate evolution (33). In the mouse, the 3 members of this family (*Msx1*, *Msx2* and *Msx3*) are expressed in the dorsal midline from early stages of neurogenesis (34–37). At the neural tube closure stage, *Msx1* expression in the CNS is restricted to the dorsal midline along its entire length (38–40). In the midline, *Msx1* is coexpressed with *Bmp* and *Wnt* genes and might therefore play a role in signaling by these diffusible molecules (40). *Msx1* homozygous mutant mice die at birth and exhibit cleft palate, an arrest in tooth development, with defects in the cranio-facial skeleton and inner ear (41, 42). The implication of *Msx* genes in ecto-mesodermal induction processes has been extensively studied (43) Moreover, despite a number of data strongly indicative of a role for *Msx* genes in the development of the CNS, little is known about their role in this structure.

In this study we used *Msx1* null mutant mice that we had produced previously to describe the main features of the CNS of mutant phenotype (42). Since the main defects are acute alterations of the SCO and the PC and the development of hydrocephalus, we discuss the role of Msx1 in SCO and PC development and the implication of these structures in the homeostasis of cerebrospinal fluid.

MATERIALS AND METHODS

Mouse Embryos

Gene targeting of the *Msx1* locus with the *nlacZ* (n, nuclear localization signal) reporter gene (*Msx1nlacZ*) was described previously (42). The *nlacZ* gene was inserted by homologous recombination in the region encoding the third helix of the *Msx1* homeodomain. This resulted in the inactivation of the gene functional domain and the formation of a fusion protein histochemically detectable by its b-galactosidase activity. This protein can be labeled in whole embryo or in slices, since it catalyses the transformation of X-Gal into a blue precipitate. Hence, the expression of the *Msx1* gene can be detected at cellular level, both in homozygous and heterozygous mutant embryos. This allele has been maintained on a C57BL/6J background. The mutant embryos were first recognized by the phenotype (i.e. primarily by detecting a cleft palate [41, 42]) and then confirmed genotypically. Homozygous, heterozygous, and wild-type embryos were distinguished by PCR using tissue from the embryo itself or from the extra-embryonic

membranes. Homozygous mutants die after birth while heterozygotes usually survive. Handling, care, and processing of the control and experimental animals were carried out according to principles approved by the Council of the American Physiological Society and national laws (B.O.E. 67, 1988, Spain).

Whole Mount b-Galactosidase Staining

E11.5 and E12.5 embryos were removed, rinsed in 0.1 M phosphate buffer saline (PBS), and fixed in 4% paraformaldehyde in PBS for 20 min. After washing twice in PBS (5 min each), embryos were put in a 0.1 M PBS solution containing 5mM potassium ferricyanide, 5 mM potassium ferrocyanide, 2 mM magnesium chloride, 0.02% Nonidet P-40 (w/v), and 400 µg/ml X-Gal (5-bromo-4-chloro-3-indolyl-beta-D-galactopyranoside) as substrate, overnight, at 328C with gentle agitation. X-Gal stocks were prepared in dimethyl sulfoxide at 40 mg/ml and stored at 2208C. Some brains were submitted to whole mount immunocytochemistry after b-galactosidase staining.

In Situ Hybridization

Msx1 antisense riboprobe was labeled with digoxigenindUTP (Boehringer Mannheim, Mannheim, Germany) by in vitro transcription of a 0.7-kb fragment-encoding mouse *Msx1* using T3 polymerase (Ambion, Austin, TX). Sense probe (using T7 polymerase) was used as control. In situ hybridization was performed on free-floating cryostat sections of paraformaldehyde-fixed embryos essentially as previously described (44, 45). Sections were prehybrided at 608C for 3 hours in a solution containing 50% formamide, 10% dextran sulfate, 5X Denhardt's solution, 0.62 M NaCl, 10 mM EDTA, 20 mM PIPES, 250 mg/ml sheared salmon sperm DNA, and 250 mg/ml yeast tRNA. Labeled riboprobe cRNA was added to the prehybridization buffer (500–1,000 ng/ml) and hybridization was performed at 608C overnight. After stringent washes, sections were incubated at 48C overnight with an anti-digoxigenin antibody conjugated to alkaline phosphatase (Roche, Barcelona, Spain) and developed with nitroblue tetrazolium (NBT) and 5-bromo-4-chloro-3-indolyl-phosphate toluidinium salt (BCIP). Tissue sections were mounted on gelatinized slides and coverslipped with Mowiol. For adults, brains were dissected out, fixed in 4% paraformaldehyde, cut using a cryostat, and processed as outlined above.

Immunocytochemical Analysis

E 18.5 wild-type (n 5 4) and mutant (n 5 7) embryos and brains from postnatal mouse (P40, n 5 4; adults n 5 2) were fixed in paraformaldehyde as described above. After being washed in PBS, they were embedded in paraffin and 10-µm coronal and sagittal sections were made. For immunocytochemistry, all steps were carried out at room temperature. Sections were first treated for 10 min with PBS containing 10% methanol and 10% hydrogen peroxide to inactivate endogenous peroxidase. After washing, they were exposed to one of the following antibodies for 18 hours: i) AFRU, the polyclonal antibody that strongly recognizes the secretory material of SCO along vertebrate phylum (4). ii) 4A6, the monoclonal antibody that selectively recognizes the secretory glycoprotein(s) of the mammals SCO (5). Immunocytochemical, immunoblot, and ELISA studies have revealed that this monoclonal antibody, among many others tested, provided the best

results for localization of SCO secretory materials (5). iii) Anti-GAP43 (GAP-7B10, mouse monoclonal, 1:1,000 dilution, Sigma, Madrid, Spain). Rabbit anti-mouse IgG (Sigma) was used as secondary antibody. All the antibodies were diluted in PBS containing 0.5% Triton X-100 and 2.5% normal serum. Sections were incubated for 45 min with the secondary antibody and diluted 1:50 in the same diluting agent as the primary antibody. After washing in buffer, the sections were incubated for 45 min at 228C with a mouse PAP (Sigma, diluted 1:200). 3,39 diaminobenzidine tetrahydrochloride (DAB, Sigma) was used as revealing agent. Omission of the primary antibody resulted in no detectable staining. Sections were counterstained with hematoxylin when required. Parallel sections of some brains were stained with hematoxylin and eosin (H&E) for a general histological description and with Alcian-blue staining for the demonstration of cartilage. Whole mount immunocytochemistry was made using anti-GAP43 after b-galactosidase staining as described for brain sections. The images in this paper were created with a digital camera and computerized using Adobe Photoshop software without modifying the content of the micrograph. The figures were prepared using Microsoft PowerPoint software.

RESULTS

The SCO of Wild-type Embryos and Adults Expresses the Msx1 Gene

We have studied the expression of *Msx1* gene either by revealing the presence of b-galactosidase in heterozygous and homozygous mutants or by in situ hybridization in wild-type specimens. We had previously established that b-galactosidase activity in the CNS of mutant embryos matched *Msx1* transcript distribution at different developmental stages (40). We have detected the secretory glycoproteins of the SCO by using a polyclonal antibody AFRU and Mab 4A6, a specific monoclonal antibody that selectively binds to the secretory material of the SCO (5). Both showed the same staining pattern and intensity. The extent of *Msx1* expression in brain structures has been described elsewhere (40). In this study we paid special attention to the region of the prosomere 1 (P1), where PC develops. The dorsal midline of the neural tube of E12.5 embryos expressed *Msx1* from the optic stalk to the tip of the tail (not shown) including P1 (Fig. 1A). The expression of *Msx1* in P1 occurs in the neuroepithelium just beneath the fiber bundles of the posterior commissure (Fig. 1B, C). This neuroepithelium begins to synthesize specific glycoproteins at about E14.5, as revealed by its immunoreactivity to antibodies against its secretory glycoprotein(s), and, therefore, from this age can be regarded as SCO (8). At E18.5, the SCO was well developed and actively secreting glycoproteins that were immunoreactive to Mab 4A6 (Fig. 1F). In situ hybridization confirmed that, at E18.5, the SCO is the region showing the highest *Msx1* expression in prosomer 1 while the surrounding ependyma is almost devoid of *Msx1* transcripts (Fig. 1D). The SCO of adult mice maintained a strong expression of *Msx1* gene (Fig. 1E) concomitantly with a high secretory activity (Fig. 1G). All parts of SCO cells contained secretory glycoproteins, including the apical and perinuclear cytoplasms and the basal processes that crossed the posterior commissure and ended in the leptomeninges (Fig. 1F, G).

The Posterior Commissure Is Affected in Msx1 Mutants

Figure 2 shows dorsal views, at the P1 level, of E11.5 embryos stained for b-galactosidase and immunostained with an antiserum against the GAP43 protein to reveal the PC fibers. In heterozygous mutants (Fig. 2A), the β-galactosidase label was present along the whole dorsal midline and the PC appeared formed by several bundles of perpendicular axons. Homozygous mutants (Fig. 2B–D) exhibited an interruption of the b-galactosidase staining of the P1 dorsal midline of variable severity, as previously described (40). Some homozygous mutants displayed a phenotype similar to the described heterozygous specimen (Fig. 2A, B). A continuous dorsal β-galactosidase labeling and the PC were visible although axonal bundles appeared thinner. A second case was a homozygous mutant that showed a weaker b-galactosidase
labeling, fewer PC fibers, and errors in fiber pathfinding (Fig. 2D). Finally, the most frequent phenotype of homozygous mutants (Fig. 2C) displayed an evident interruption in the b-galactosidase staining domain at the prospective P1 that showed very few PC fibers. These data show a correlation between the extent of midline *Msx1* expression interruption and the degree of disorganization of the PC.

Phenotype of Homozygous E18.5 Msx1nlacZ/nlacZ Mutants

To perform a detailed histological study we sectioned and stained wild-type specimens and homozygous and heterozygous mutants at E18.5 and P40. Most E18.5 homozygous mutants (5 of 7 studied) showed absence of SCO and PC as well as aqueductal collapse and hydrocephalus. In 2 of 7 mutants, a PC was present as well as an underlying thick ependymal structure that highly resembled the SCO as depicted after the use of unspecific histological dyes. We first describe the most frequent phenotype of homozygous mutants. This mutant phenotype corresponded to that shown in Figure 2C, having absence of b-galactosidase staining in the region of P1 just beneath the prospective PC. The most conspicuous malformation was the lack of P1 derivatives SCO and the PC. This is quite clearly seen in sagittal sections (Fig. 3B, D, F). In the anatomical region where the SCO should be present, a monolayer ependyma was found but no morphological or immunocytochemical signs of a SCO were evident. The SCO of wild-type mice were characterized by a thick prismatic ependyma with long basal processes that showed strong immunoreactivity (Figs. 1E, 3A, C). None of these characteristics could be seen in the corresponding region of homozygous mutants (Fig. 3B, D, F). PC was absent in these mutants. However, few crosssectioned axonal bundles could be detected beneath the ependyma of this region (Fig. 3F insets). These bundles could correspond to the few fibers seen in whole mount preparations of younger embryos (Fig. 2C). Another characteristic of null mutants was the absence of an open aqueduct. In none of the specimens studied missing the PC and the SCO was the aqueduct open. It was always collapsed at its rostral region, anterior to the collicular recess (compare Fig. 3B, D, F with Fig. 3A, C, E and Fig. 4H, I, M with Fig. 4K, L, P). The ependymal walls both sides approached and no lumen could be seen between them. In the periaqueductal region, pyknotic nuclei surrounded by a clear cytoplasmic halo were frequent (Fig. 5D). In wild-type mice, although a certain degree of collapse was normal in the ventral region of the aqueduct as

seen in transverse sections, there was always an open region dorsally just beneath the subcommissural organ (Fig. 4M, inset). In mutants, the absence of SCO was accompanied by the occlusion of this lumen (Fig. 4P inset). There was no difference with respect to the collicular recess, the caudal aqueduct, or the fourth ventricle (Fig. 3A, B). Other circumventricular organs of the dorsal midline showed morphological differences as compared with wild-type mice. The pineal gland of E18.5 wild-type mice appeared as a solid structure rostral to the SCO and attached to the diencephalic roof by the pineal stalk (Figs. 3A, 4I). In mutants, an anomalous undeveloped pineal gland was located in the proximity of the wall of an expanded pineal recess in continuity with the third ventricle (Figs. 3B, 4L). The anterior choroid plexus of mutants looked normal under the light microscope. The subfornical organ (located beneath the fornix) was reduced in mutants as depicted in sagittal and transverse sections (compare Fig. 3A with 3B and Fig. 4B with 4E).

Hydrocephalus was one of the most conspicuous features and fully penetrant of the homozygous mutant phenotype and affected both lateral ventricles and the third ventricle (Figs. 3, 4). Together with hydrocephalus, a thinning of the cortical mantle and a smaller hippocampus and fornix were seen in mutants (Fig. 4). We did not observe significant differences in the size of the corpus callosum, the anterior commissure, and the habenular commissure (Figs. 3, 4). Sometimes, edema and subventricular cavitations were found, especially in the rostral horn of the lateral ventricles. Another characteristic event occurring in E18.5 homozygous mutants was denudation of the ependymal layer in a region located in the dorsal third ventricle next to the opening of the foramen of Monroe (Fig. 4F). In this region, supraependymal cells were frequent. Also the presence of a cartilaginous bar in the caudal region of the interhemispheric wall, identified after Alcian-blue staining, was typical in mutants (Fig. 4J, insets).

As described above, the phenotype of homozygous mutants was not fully penetrant. Although most of the specimens studied lacked structures derived from prosomere 1, some specimens displayed PC and a thick subjacent pseudostratified ependyma that, using unspecific dies, looked similar to that of the SCO (Fig. 5A). In paraffin sections of homozygous mutants having a structure with the morphology of an SCO, the monoclonal antibody 4A6 stained only very few individual ependymal cells of the region, the vast majority of them being negative (Fig. 5B). Fibers of the posterior commissure were positive to antibodies against GAP43 (Fig. 5C). The aqueduct was collapsed and no lumen was visualized, in addition, pyknotic nuclei in the periaqueductal region were numerous (Fig. 5D). Hydrocephalus was evident in 1 of 2 specimens studied having this phenotype.

Phenotype of Heterozygous Msx1$^{+/nlacZ}$ Mutants

The phenotype of heterozygotes varied from being almost indistinguishable to that of wild-type mice to animals showing severe defects in P1 derivatives. About one third of the heterozygotes studied showed hydrocephalus.

In whole mount preparations of heterozygous mutant embryos, β-galactosidase staining was observed in P1 and fibers of the PC were seen as negative bands crossing the stained region (Figs. 1A, 2A). Since most heterozygotes survived, we describe the phenotype of P40 mice that showed hydrocephalus and strong alterations of the SCO.

In all of these animals, the SCO was present and immunoreactive to 4A6. However, its size was about half the size of a wild-type SCO. Whereas the immunoreactive SCO of P40 wild-type specimens extended rostrocaudally for about 500 μm, the SCO of heterozygotes occupied no more than 250 μm (Fig. 6A, B). This size reduction was also evident in transverse sections where the SCO of heterozygous was also half the size of wildtype SCO (Fig. 6C, D insets). The PC was present in heterozygous mutants and, in contrast to SCO, its size was similar to that of wild-type. The caudal region of the SCO of heterozygotes was quite disorganized (Fig. 6H) compared to wild-type (Fig. 6F) and showed digitations, branches (Fig. 6B), and rosettes, some displaying 4A6-immunoreactive cells (Fig. 6H). An open rostral aqueduct similar to that seen in wild-type (Fig. 6G) was never observed in heterozygotes with phenotypes of this type. The ependymal wall from both sides of the aqueduct approached and no lumen was visible (Fig. 6I). The most prominent feature of these mutant specimens was severe hydrocephalus. The lateral ventricles were dramatically enlarged (compare Fig. 6C with 6D, both at the same magnification) and most of the wall surfaces were devoid of ependyma (Fig. 6D inset). The thinning of the cortical mantle was maximal and in some places virtually no neuronal tissue was present between the ventricular wall and the meninges (Fig. 6D). In the ventricle, flocculent materials and cellular elements and debris were present. Also, it was not uncommon to find erythrocytes. In the rostral lateral ventricles, subventricular cavitations and edemas were abundant, as well as what appeared to be distended subventricular blood vessels (Fig. 6E). Hydrocephalus was restricted to the lateral and the third ventricles.

DISCUSSION

The Expression of Msx1 Is Necessary for the Development of Structures Derived of the Dorsal Midline of Prosomere 1 Two structures derived from the dorsal midline of P1 are the SCO and the PC (46). During embryonic development, several regulatory genes are expressed in this region at different time periods and with a specific spatial distribution (1). Absence of expression of some of these genes or ectopic expression in P1 of regulatory factors normally restricted to neighboring territories leads to the absence or malformation of the SCO and the PC (see Introduction). Recently, it has been stated that the borderline between the diencephalon and mesencephalon is established by a series of inductive and repulsive interactions of several regulatory genes, among which *Pax6*, *Pax2*, *Pax5*, and *En1* are of crucial importance (47). Thus, it seems that the development of PC and SCO depends on the expression of regulatory genes in P1 and the neighboring regions.

Msx1 is a regulatory gene involved in epithelio-mesenchymal interactions at sites of embryonic induction, such as in the developing limbs (43). Although *Msx1* expression extends along the entire length of the CNS dorsal midline (38, 39), in mutants we found the most dramatic effects in P1 derivatives SCO and PC that virtually did not develop. Thus, in addition to other regulatory genes, the development of SCO and PC depends on the expression of *Msx1*.

Although most homozygous *Msx1* mutants lacked SCO and PC, a few specimens displayed both structures. It is known that, in addition to *Msx1*, the *Msx2* gene is expressed at E10.5 in the dorsal P1, but weakly, and is downregulated at E12.5 (40). Furthermore, it has been reported that Msx1 and Msx2 proteins exhibit similar DNA binding properties and function (35). Hence, it is likely that the absence of the Msx1 protein is partially compensated by Msx2. However, in these few homozygous mutants displaying a structure morphologically similar to SCO, compensatory mechanisms do not seem to be complete since only very few SCO cells show the characteristics that define SCO cells, namely, the capacity to secrete specific glycoproteins. The presence of this type of specimens demonstrates that expression of *Msx1* is needed not only for the formation of the SCO primordium but also for the specific secretory activity of the functional SCO, and that the presence of these specific secretory glycoproteins do not seem to be necessary for the development of the PC (see later). The necessity of *Msx1* expression for SCO glycoprotein secretion was also reflected by the high *Msx1* expression of the adult SCO.

How *Msx1* expression affects CNS development is not presently known, however, some reports reveal interesting clues. It has been shown that *Msx1* is coexpressed with *Bmp* and *Wnt* genes (40, and references therein) and thus the effects observed in mutants could be related to changes in the production of these diffusible molecules. Significantly, BMP signaling has been demonstrated in the regulation of the expression boundaries of the homeobox proteins Pax6 and Msx1 during the development of the dorsal neural tube (48), allowing us to hypothesize a similar relationship in the dorsal P1 development. On the other hand, it has been reported that *Msx1* and *Msx2* regulate cadherin-mediated cell adhesion and cell sorting (49) and selective expression of cadherins define CNS territories (50). A normal mouse SCO development correlates with expression of R-cadherin and OB-cadherin (8); therefore it is possible that the absence of SCO development in *Msx1* mutants could be related to changes in the pattern of cadherin expression. It has also been shown that the amount of connexin43 protein was associated with the level of *Msx1* expression (51). Connexin43 forms gap-junctions that are of importance for the activity of the SCO (52).

The Secretory Activity of the SCO Depends on the Amount of Msx1 Protein

From the above data, the presence of Msx1 protein seems to be necessary for the secretory activity of the SCO. In spite of the presence of a structure that morphologically resembles the SCO beneath the PC of some homozygous mutants, the vast majority of its ependymal cells were negative to a specific monoclonal antibody that identifies rodent SCO secretory glycoproteins (5). The possibility exists that these specimens synthesize a modified form of SCO-glycoprotein that lack the epitope recognized by Mab 4A6. Thus, we used a polyclonal antiserum (AFRU) that recognized a wide spectrum of epitopes and other monoclonal antibodies raised in our laboratory (5, results not shown) with exactly the same results in all cases. These evidences indicate that very probably SCO specific glycoproteins are absent in *Msx1* homozygous mutants.

Heterozygous mutants displayed a range of SCO phenotypes varying from almost normal to highly reduced. This fact could be the consequence of 2 factors: 1) genetic

redundancy with Msx2, as has been discussed above, and 2) dose dependence. The most frequent heterozygous phenotype showed a reduced secretory SCO. Since heterozygous mutants produce half the amount of Msx1 functional protein, the number of secretory cells in the SCO could depend directly on the amount of Msx1 protein present in the cells.

Expression of SCO-Glycoproteins and the Formation of PC

As discussed above, the development of SCO and PC depend on *Msx1* (and/or *Msx2*) gene expression. We never found a PC without SCO or vice-versa, which was also true in *small eye* mutants (8). A putative involvement of SCO secretory glycoproteins in PC development of the posterior commissure was suggested based upon 2 facts: i) The SCO seems to release secretory molecules at its basal pole, including the basal processes protruding among the fiber bundles of the PC (53); and ii) SCO specific glycoproteins exert, in vitro, an important influence on neuronal adhesion and neurite extension (14, 15, 54). However, according to our results, some *Msx1* homozygous mutants displayed a PC over an SCO that did not have specific SCO secretory glycoproteins, as depicted after the use of specific antibodies. This indicates that SCO secretory glycoproteins are not essential for the formation of PC and is supported by other evidence. In the mouse, axonal bundles of the PC are visible from E10.5 (9), whereas the SCO starts synthesizing glycoproteins at about E14.5 (8). Moreover, mutant mice lacking the transcription factor RFX4pv3 fail to develop SCO, although PC is present (55). It is, however, feasible that the dorsal midline neuroepithelium of the prosomer 1, either before or during SCO development, could be the origin of still unidentified axonal guidance molecules involved in the formation of PC.

SCO Defects Are Related to Aqueductal Stenosis and Hydrocephalus in Mutants

According to our results, the absence of SCO and PC in *Msx1* mutants was linked to alterations and collapse of the aqueductal wall and hydrocephalus. Even in heterozygous mutants with a partially developed SCO, the aqueduct showed important defects. Several reports demonstrate the requirement of a functional SCO for the development of the aqueduct and hence for the prevention of obstructive hydrocephalus. Evidence can be classified into 3 groups. A first group is formed by rodent strains carrying spontaneous mutations, such as the SUMS/NP mouse (23), the H-Tx rat (25), the MT/HokIdr mouse (21), the CWS/Idr rat (22), and the *hyh* mouse (27). A second group is composed of mouse mutants for regulatory genes, such as *Pax6* (8), *Msi1* (20), *Wnt1*, the transcription factor RFX4pv3 (55) and ectopic *En1* (17). A third group comprises experimental models such as newborn rats from mothers fed with vitamin B12- or folic acid-deficient diets (30, 31) and from X-irradiated mothers (29). All these studies point to the same conclusions: defects in the formation of the SCO lead to obstruction in the aqueduct and hydrocephalus. In accordance with this proposal, it has been reported that immunoneutralization of the SCO of developing rats by maternal transfer of antibodies led to stenosis of the aqueduct and a consequent hydrocephalus (32). Thus, it has been proposed that the specific glycoproteins released by the SCO into the cerebrospinal fluid of the third ventricle are responsible for the maintenance of an open aqueduct. Accordingly, most homozygous *Msx1* mutants that lacked SCO displayed aqueductal

stenosis and hydrocephalus. Interestingly, the few homozygous *Msx1* mutants that showed a PC and a structure resembling SCO also suffered from aqueductal stenosis and hydrocephalus. In these animals, the SCO did not produce any specific glycoprotein recognized by the antibodies used. This reinforces the hypothesis that not only the presence of a SCO structure, but also the presence of specific SCO glycoproteins in the CSF, is necessary for the maintenance of an open aqueduct.

By which mechanism SCO-specific glycoprotein(s) prevents aqueductal collapse and hydrocephalus is not known. SCO-spondin (14) and RF-Gly I (56), the 2 characterized SCO glycoproteins, show repeated sequences that could be responsible for the aggregative or anti-aggregative properties displayed by RF glycoproteins in vitro (54). On the other hand, it has been reported that rats with an immunoneutralization of the SCO display increased levels of monoamines in the cerebrospinal fluid (57) and monoamines participates in the control of cerebrospinal fluid production (58). Moreover, it was shown that choroid plexus have binding sites for SCO glycoproteins (59) and hence they could influence its function.

From the above data, it can be proposed that the development of hydrocephalus in *Msx1* mutants is due to obstruction of cerebrospinal fluid (CSF) transit through the aqueduct. In addition, other features seen in mutants could favor the appearance and severity of this pathology. Under normal circumstances, about 20% of the CSF is produced by capillary filtration from the nervous parenchyma and reaches the ventricular CSF through spaces between the ependymal cells (60). Permeability through intercellular spaces among the ependymal cells has been reported to depend on mannose-containing glycoconjugates and lectins (61, 62). Thus the absence of ependyma, as described in *Msx1* mutants, could lead to increasing production of parenchymal CSF. This has been reported to be the primary cause of congenital hydrocephalus in developing *Hyh* rats (63). In these animals, ependymal denudation and hydrocephalus preceded aqueductal stenosis. In agreement with this idea we reported that experimental ependymal denudation in adult rats led to severe hydrocephalus (64). Another feature of *Msx1* mutants that could contribute to the development of hydrocephalus are subventricular cavitations and edemas found in the rostral lateral ventricle. In other animal models these features have also been described in the rostral lateral ventricle (20).

In this report we have described a number of alterations found in *Msx1* mutants, including reduced subfornical organ and a modified pineal gland. The presence of an ectopic cartilaginous bar in the inter-hemispheric wall could be considered a skeletal defect in addition to others known to occur in the craniofacial bones of *Msx1* mutants (42).

ACKNOWLEDGMENTS

We acknowledge the skillful technical work of Jose Esteban Casares Mira.

REFERENCES

1. Rubenstein JL, Martinez S, Shimamura K, Puelles L. The embryonic vertebrate forebrain: The prosomeric model. Science 1994; 266:57880

2. Rodrı´guez EM, Rodríguez S, Hein S. The subcommissural organ. Microsc Res Tech 1998;41:98–123.

3. Reissner E. Beiträge zur Kenntnis vom Bau des Rückenmarks von *Petromyzon fluviatilis*. L Arch Anat Physiol 1860;77:545–88

4. Rodríguez EM, Oksche A, Hein S, Rodríguez S, Yulis C. Comparative immunocytochemical study of the SCO. Cell Tissue Res 1984; 237:427–41

5. Fernández-Llebrez P, Miranda E, Estivill-Torrús G, et al. Analysis and quantification of the secretory products of the subcommissural organ by use of monoclonal antibodies. Microsc Res Tech 2001; 52:510–19

6. Schöebitz K, Garrido O, Heinrichs M, Speer L, Rodríguez EM. Ontogenetical development of the chick and duck SCO. Histochemistry 1986;84:31–40

7. Schöebitz K, Rodríguez EM, Garrido O, del Brio-León MA. Ontogenetic development of the SCO with reference to the flexural organ. In: Oksche A, Rodrı´guez EM, Ferna´ndez-Llebrez P, eds. The SCO. An ependymal brain gland. New York: Springer, 1993:41–49

8. Estivill-Torrús G, Vitalis T, Fernández-Llebrez P, Price DJ. The transcription factor Pax6 is required for development of the diencephalic dorsal midline secretory radial glia that forms the subcommissural organ. Mech Dev 2001;109:215–24

9. Mastick GS, Easter SS Jr. Initial organization of neurons and tracts in the embryonic mouse fore- and midbrain. Dev Biol 1996;173: 79–94

10. Monnerie H, Dastugue B, Meiniel A. Reissner's fibre promotes neuronal aggregation and influences neuritic outgrowth in vitro. Cell Tissue Res 1997;281:285–95

11. Klar A, Baldassare M, Jessell TM. *F-spondin*: A gene expressed at high levels in the floor plate encodes a secreted protein that promotes neural cell adhesion and neurite extension. Cell 1992;69:95–110

12. Higashijima S, Nose A, Eguchi G, Hotta Y, Okamoto H. Mindin/ F-spondin family: Novel ECM proteins expressed in the zebrafish embryonic axis. Dev Biol 1997;192:211–27

13. Burstyn-Cohen T, Tzarfaty V, Frumkin A, Feinstein Y, Stoeckli E, Klar A. F-Spondin is required for accurate pathfinding of commissural axons at the floor plate. Neuron 1999;23:233–46

14. Gobron S, Monnerie H, Meiniel R, et al. SCO-spondin: A new member of the thrombospondin family secreted by the SCO is a candidate in the modulation of neuronal aggregation. J Cell Sci 1996;109:1053–61

15. Gobron S, Creveaux I, Meiniel R, et al. SCO/Reissner's fiber complex: Characterization of SCO-spondin, a glycoprotein with potent activity on neurite outgrowth. Glia 2000;32:177–91

16. Schwarz M, Alvarez-Bolado G, Dressler G, Urba´nek P, Busslinger M, Gruss P. *Pax2/5* and *Pax6* subdivide the early neural tube into three domains. Mech Develop 1999;82:29–39

17. Louvi A, Wassef M. Ectopic *engrailed 1* expression in the dorsal midline causes cell death, abnormal differentiation of circumventricular organs and errors in axonal pathfinding. Development 2000;127:4061–71
18. Stoykova A, Fritsch R, Walther C, Gruss P. Forebrain patterning defects in *Small eye* mutant mice. Development 1996;122:3453–65
19. Thomas KR, Capecchi MR. Targeted disruption of the murine *int-1* proto-oncogene resulting in severe abnormalities in midbrain and cerebellar development. Nature 1990;346:847–50
20. Sakakibara S, Nakamura Y, Yoshida T, et al. RNA-binding protein Musashi family: Roles for CNS stem cells and a subpopulation of ependymal cells revealed by targeted disruption and antisense ablation. Proc Natl Acad Sci USA 2002;99:15194–99
21. Takeuchi IK, Kimura R, Matsuda M, Shoji R. Absence of subcommissural organ in the cerebral aqueduct of congenital hydrocephalus spontaneously occurring in MT/HokIdr mice. Acta Neuropathol (Berl) 1987;73:320–22
22. Takeuchi IK, Kimura R, Shoji R, Matsuda M. Dysplasia of subcommissural organ in congenital hydrocephalus spontaneously occurring in CWS/Idr rats. Experientia 1988;44:338–40
23. Jones HC, Dack S, Ellis C. Morphological aspects of the development of hydrocephalus in a mouse mutant (SUMS/NP). Acta Neuropathol (Berl) 1987;72:268–76
24. Bruni JE, del Bigio MR, Cardoso ER, Persaud TVN. Hereditary hydrocephalus in laboratory animals and humans. Exp Pathol 1988; 35:239–46
25. Jones HC, Bucknall RM. Inherited prenatal hydrocephalus in the *H-Tx* rat: A morphological study. Neuropathol Appl Neurobiol 1988;14:263–74
26. Yamada H, Oi S, Tamaki N, Matsumoto S, Sudo K. Histological changes in the midbrain around the aqueduct in congenital hydrocephalic rat LEW/Jms. Childs Nerv Syst 1992;8:394–98
27. Pérez-Fígares JM, Jiménez AJ, Pérez-Martín M, et al. Spontaneous congenital hydrocephalus in the mutant mouse *hyh*. Changes in the ventricular system and the subcommissural organ. J Neuropathol Exp Neurol 1998;57:188–202
28. Castañeyra-Perdomo A, Meyer G, Carmona-Calero E, et al. Alterations of the subcommissural organ in the hydrocephalic human fetal brain. Dev Brain Res 1994;79:316–20
29. Takeuchi IK, Takeuchi YT. Congenital hydrocephalus following Xirradiation of pregnant rats on an early gestational day. Neurobehav Toxicol Teratol 1986;8:143–50
30. Overholser MD, Whitley JR, O'Dell BL, Hogan AG. The ventricular system in hydrocephalic rat brains produced by a deficiency of vitamin B12 or folic acid in the maternal diet. Anat Rec 1954; 120:917–23
31. Newberne PM. The subcommissural organ of the vitamin B12-deficient rat. J Nutrition 1962;76:393–413
32. Vio K, Rodríguez S, Navarrete EH, Pérez-Fígares JM, Jiménez AJ, Rodríguez EM. Hydrocephalus induced by immunological blockage of the subcommissural organ-Reissners fiber (RF) complex by maternal transfer of anti-RF antibodies. Exp Brain Res 2000;135: 41–52

33. Sharman AC, Shimeld SM, Holland PW. An amphioxus *Msx* gene expressed predominantly in the dorsal neural tube. Dev Genes Evol 1999;209:260–63
34. Robert B, Sassoon D, Jacq B, Gehring W, Buckingham M. *Hox-7*, a mouse homeobox gene with a novel pattern of expression during embryogenesis. Embo J 1989;8:91–100
35. Catron KM, Wang H, Hu G, Shen MM, Abate-Shen C. Comparison of *Msx1* and *Msx2* suggests a molecular basis for functional redundancy. Mech Dev 1996;55:185–99
36. Shimeld SM, McKay IJ, Sharpe PT. The murine homeobox gene *Msx-3* shows highly restricted expression in the developing neural tube. Mech Dev 1996;55:201–10
37. Wang W, Chen X, Xu H, Lufkin T. *Msx3*: A novel murine homologue of the Drosophila *msh* homeobox gene restricted to the dorsal embryonic central nervous system. Mech Dev 1996;58:203–15
38. Liem KFJ, Tremml G, Roelink H, Jessell TM. Dorsal differentiation of neural plate cells induced by BMP-mediated signals from epidermal ectoderm. Cell 1995;82:969–79
39. Furuta Y, Piston DW, Hogan BL. Bone morphogenetic proteins (BMPs) as regulators of dorsal forebrain development. Development 1997;124:2203–12
40. Bach A, Lallemand Y, Nicola MA, et al. *Msx1* is required for dorsal diencephalons patterning. Development 2003;130:4025–36
41. Satokata I, Maas R. *Msx1* deficient mice exhibit cleft palate and abnormalities of craniofacial and tooth development. Nat Genet 1994;6:348–56
42. Houzelstein D, Cohen A, Buckingham ME, Robert B. Insertional mutation of the mouse *Msx1* homeobox gene by an *nlacZ* reporter gene. Mech Dev 1997;65:123–33
43. Davidson D. The function and evolution of *Msx* genes: Pointers and paradoxes. Trends Genet 1995;11:405–11
44. de Lecea L, Soriano E, Criado JR, Steffensen SL, Henriksen SJ, Sutcliffe JG. Transcripts encoding a neural membrane CD26 peptidase- like protein are stimulated by synaptic activity. Mol Brain Res 1994;25:286–96
45. de Lecea L, Del Río JA, Criado JR, et al. Cortistanin is expressed in a distinct subset of cortical interneurons. J Neurosci 1997;17: 5868–80
46. Figdor MC, Stern CD. Segmental organization of embryonic diencephalons. Nature 1994;363:630–34
47. Matsunaga E, Araki I, Nakamura H. *Pax6* defines the di-mesencephalic boundary by repressing *En1* and *Pax2*. Development 2000; 127:2357–65
48. Timmer JR, Wang C, Nisswander L. BMP signalling patterns the dorsal and intermediate neural tube via regulation of homeobox and helix-loop-helix transcription factors. Development 2002;129: 2459–72
49. Lincecum JM, Fannon A, Song K, Wang Y, Sassoon DA. *Msh* homeobox genes regulate cadherin-mediated cell adhesion and cell sorting. J Cell Biochem 1998;70:22–28
50. Redies C, Ast M, Nakagawa S, Takeichi M, Martı´nez-de-la-Torre M, Puelles L. Morphologic fate of diencephalic prosomeres and their subdivisions revealed by mapping cadherin expression. J Comp Neurol 2000;421:481–514
51. McGonnell IM, Green CR, Tickle C, Becker DL. Connexin43 gap junction protein plays an essential role in morphogenesis of the embryonic chick face. Dev Dyn 2001;222:420–38

52. González CA, Garcés G, Sáez JC, Schöebitz K, Rodríguez EM. The ependymocytes of the bovine subcommissural organ are functionally coupled through gap junctions. Neurosci Lett 1999;262:175–78
53. Fernández-Llebrez P, Pérez J, Nadales AE, Pérez-Fígares JM, Rodríguez EM. Vascular and leptomeningeal projections of the subcommissural organ of reptiles. Lectin histochemical, immunocytochemical and ultrastructural studies. Histochemistry 1987;87:607–14
54. Meiniel A. SCO-spondin, a glycoprotein of the subcommissural organ/Reissners fiber complex: Evidence of a potent activity on neuronal development in primary cell cultures. Microsc Res Tech 2001;52:484–95
55. Blackshear PJ, Graves JP, Stumpo DJ, Cobos I, Rubenstein JLR, Zeldin DC. Graded phenotypic response to partial and complete deficiency of a brain-specific transcript variant of the winged helix transcription factor RFX4. Development 2003;130:4539–52
56. Nualart F, Hein S, Yulis RC, Zárraga AM, Araya A, Rodríguez EM. Partial sequencing of Reissners fiber glycoprotein I (RF-Gly I). Cell Tissue Res 1998;292:239–50
57. Rodríguez S, Vio K, Wagner C, et al. Changes in the cerebrospinalfluid monoaminesin rats with an immunoneutralization of the subcommissural organ-Reissners fiber complex by maternal delivery of antibodies. Exp Brain Res 1999;128:278–90
58. Lindvall M, Edvinsson L, Owman C. Sympathetic nervous control of cerebrospinal fluid production from the choroid plexus. Science 1978;201:176–78
59. Miranda E, Almonacid JA, Rodrı´guez S, et al. Searching for specific binding sites of the secretory glycoproteins of the subcommissural organ. Microsc Res Tech 2001;52:541–51
60. Davson H, Segal MB. Physiology of the CSF and blood-brain barriers. Boca Rato´n, FL: CRC Press, 1996
61. Perraud F, Kuckler S, Gobaille S, Labourdette G, Vincendon G, Zanetta JP. Endogenous lectin CSL is present on the membrane of cilia of rat ependymal cells. J Neurocytol 1988;17:745–52
62. Kuchler S, Graff MN, Gobaille S, et al. Mannose dependent tightening of the rat ependymal cell barrier. In vivo and in vitro study using neoglycoproteins. Neurochem Int 1994;24:43–55
63. Jiménez AJ, Tomé M, Páez P, et al. A programmed Ependymal denudation occurring during the embryonic life precedes the development of congenital hydrocephalus in the mutant mouse *hyh*. J Neuropathol Exp Neurol 2001;60:1105–19
64. Grondona JM, Pérez-Martín M, Cifuentes M, et al. Ependymal denudation, aqueductal obliteration and hydrocephalus after a single injection of neuraminidase into the cerebral ventricle of adult rats. J Neuropathol Exp Neurol 1996;55:1000–1100

FIGURES

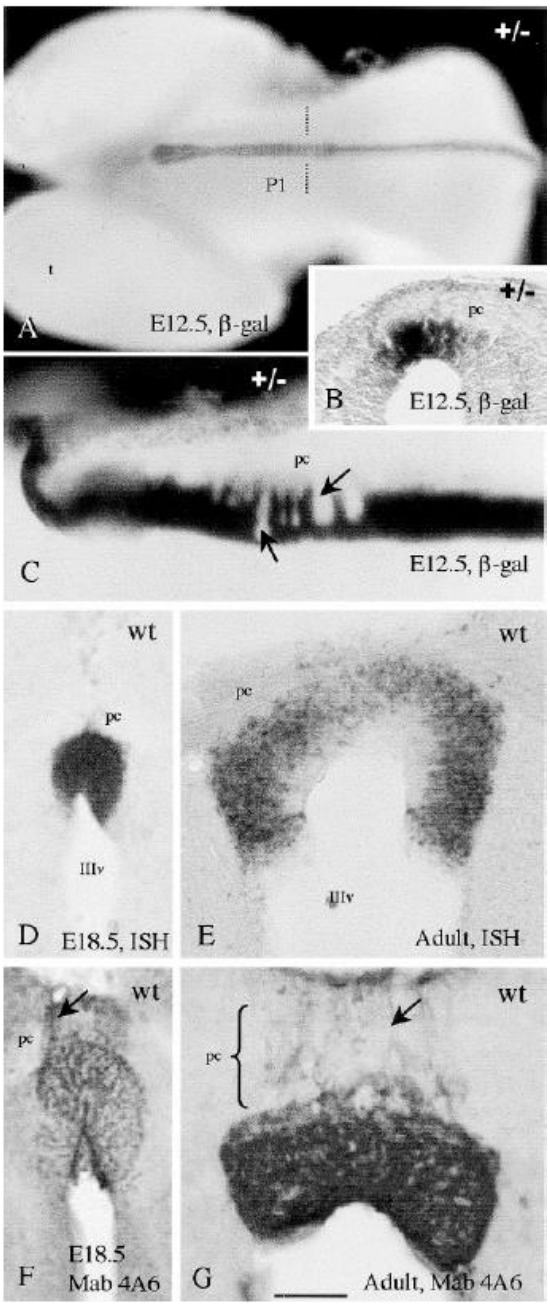

Fig. 1. *Msx1* is expressed in the subcommissural organ. **A:** Brain of E12.5 *Msx1*$^{+/nlacZ}$ heterozygous embryo stained for β-galactosidase. *Msx1* expression domain extends over the dorsal midline in the whole P1 and caudalward. Note that in P1, lighter strands that correspond to unstained fibers of the posterior commissure crossing the midline (see panel C). **B:** Transverse section of E12.5 heterozygous embryo brain stained for b-galactosidase and counterstained with H&E through a region similar to that indicated by the dotted line in the preceding figure. The region stained beneath the posterior commissure (pc) corresponds to the developing subcommissural organ. **C:** Sagittal section through P1 roof of the brain shown in panel A. Fiber bundles of the posterior commissure (pc) intermingled among the b-galactosidase-stained neuroepithelium (arrows) that

correspond to the developing subcommissural organ. This anatomical disposition led to the light strands described in panel A. **D, E:** Transverse sections through the subcommissural organ of wild-type E18.5 embryo and adult, respectively, stained by in situ hybridization for Msx1 mRNA. Abbreviations: pc, posterior commissure; IIIV, third ventricle. **F, G:** Transverse sections through the subcommissural organ of wild-type E18.5 embryo and adult, respectively, stained by immunocytochemistry using the monoclonal antibody 4A6 that selectively recognizes the secretory glycoproteins of the SCO. Note immunoreactive basal processes of SCO ependymal cells (arrows) crossing the posterior commissure (pc). The calibration bar in panel G applies to panels A (500 µm); B and C (80 µm); and D–G (100 µm).

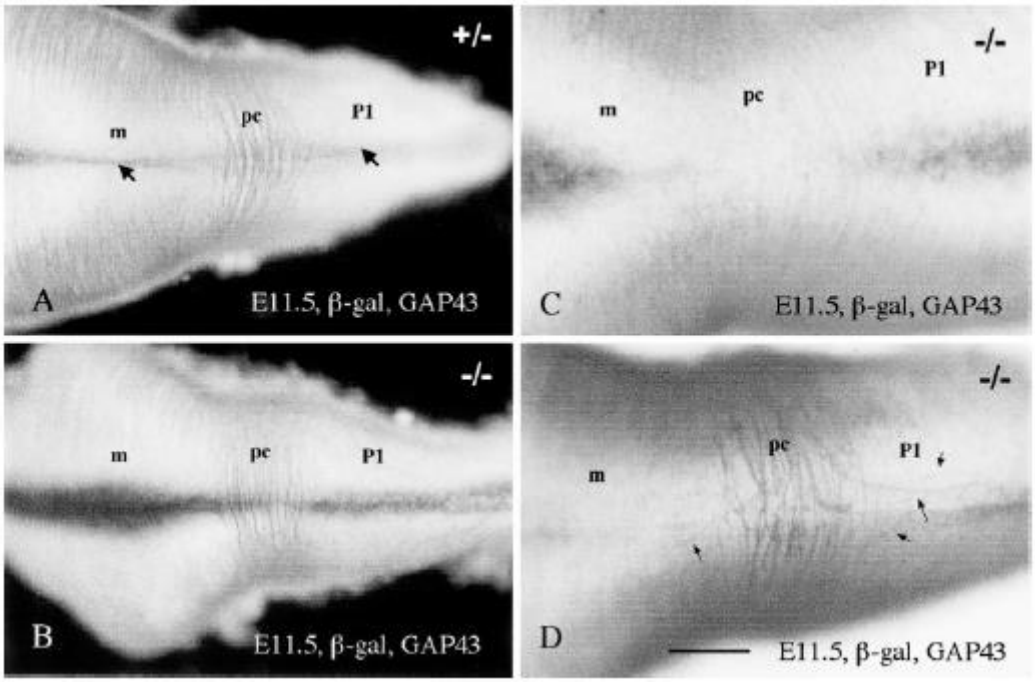

Fig. 2. The degree of development of the PC varies in different mutants and is related to the presence of an underlying neuroepithelium. **A–D:** Whole mount E11.5 embryos doubly labeled for b-galactosidase and antibodies against the axonal protein GAP43. **A:** This heterozygous shows a well-developed posterior commissure (pc) over the b-galactosidase-stained neuroepithelium (arrows). **B–D:** These 3 homozygous mutants show different degrees in the development of the posterior commissure (pc), but in all cases the paucity of fiber tracts and the presence of misconducted fibers **(D,** arrows) is related to the intensity of βgalactosidase staining. Abbreviations: P1, P1 prosomere; m, mesencephalon. The calibration bar in panel D applies to all panels (300 µm).

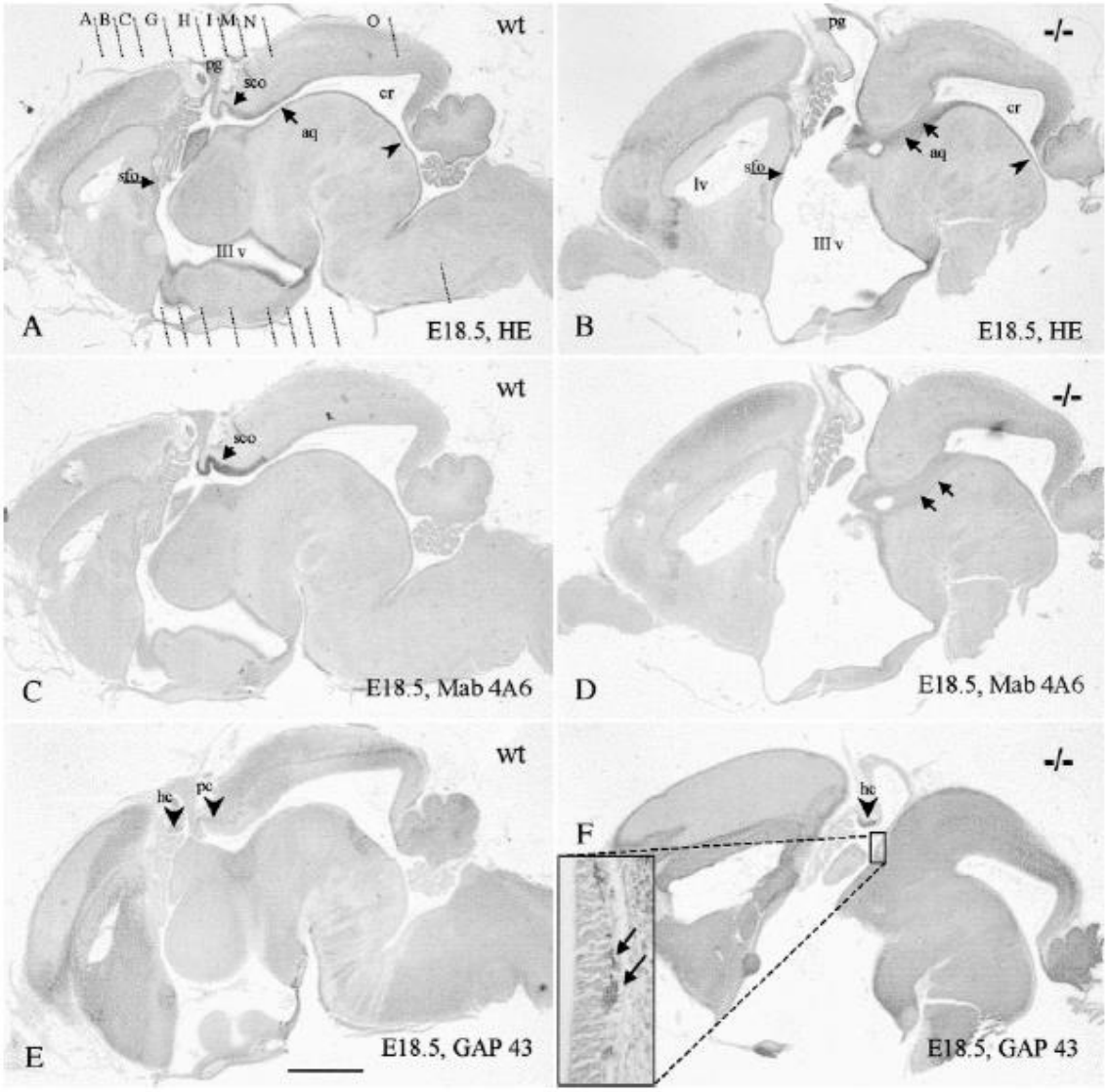

Fig. 3. The subcommissural organ and the posterior commissure are absent in homozygous mutants. Mid-sagittal paraffin sections through the brains (E18.5) of a wild-type **(A, C, E)** and a homozygous mutant *Msx1*$^{nlacZ/nlacZ}$ **(B, D, F)** stained with H&E **(A, B)**, the monoclonal antibody 4A6 that recognizes the secretory material of the subcommissural organ **(C, D)** and the monoclonal antibody GAP43 that recognizes axonal bundles **(E, F)**. Although wild-type animals have a prominent subcommissural organ (sco) and posterior commissure (pc), both structures are absent in this mutant. **F, inset:** Details of the region where presumptively the SCO should be present; cross-sectioned fiber bundles are present beneath the local neuroepithelium (arrows). In mutants, hydrocephalus is evident in the lateral ventricles (lv) and third ventricle (IIIv) but not in the collicular recess (cr). The pineal gland is present, lining the wall of an enlarged pineal recess. Although an open rostral aqueduct is evident in wildtype (aq), we never seen an aqueductal lumen in any of the serial sagittal sections done in mutants. However, the caudal part of the aqueduct is present in both (**A, B,** arrowheads). Levels indicated in panel A correspond with the transverse sections shown in Figure 4.

Abbreviations: hc, habenular commissure; sfo, subfornical organ. The calibration bar in panel E applies to all panels (500 µm) and to inset (80 µm).

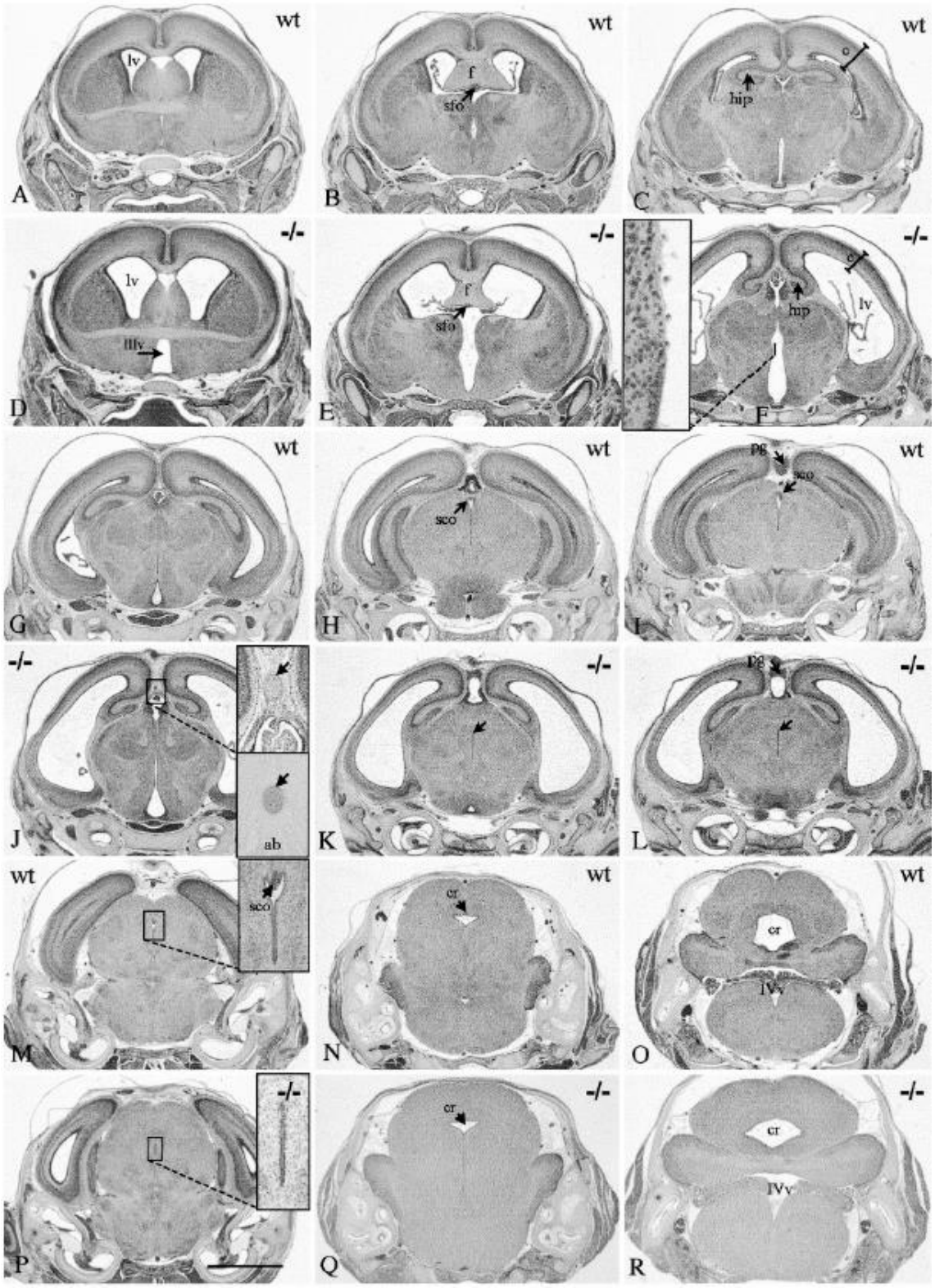

Fig. 4. Phenotype of the brain of homozygous mutant *Msx1nlacZ/nlacZ*. Representative transverse sections through the brain of E18.5 wild-type **(A–C, G–I, M–O)** and homozygous mutant *Msx1nlacZ/nlacZ* **(D–F, J–L, P–R)** at the levels indicated in Figure 3A stained with H&E. Hydrocephalus is evident in the lateral ventricle (lv) and third ventricle (IIIv) but not in the collicular recess (cr) or the fourth ventricle (IVv). Total obliteration of the rostral aqueduct occurs in mutants (**K, L,** arrows; **P, inset**). The fórnix (f), subfornical organ (sfo), cortex (c), and hippocampus (h) are smaller in mutants **(B, C, E, F)**. In mutants, ependymal denudation occurs in a region of the dorsal half of the lateral wall of the third ventricle **(F, inset)** and a cartilaginous body stained by Alcianblue dye (ab) is present in the caudal interhemispheric region (**J, inset,** arrows). The calibration bar in panel P applies to all panels (1,300 µm) and to insets (300 µm).

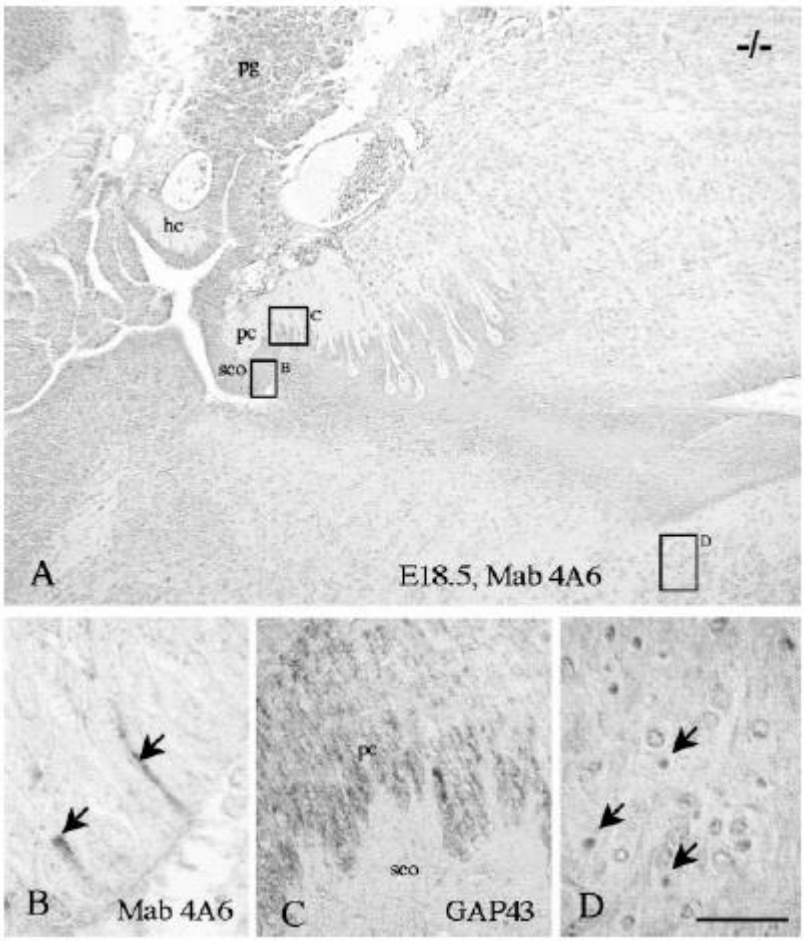

Fig. 5. Some homozygous mutants develop a posterior commissure. **A:** Sagittal section through the dorsal diencephalon of an E18.5 homozygous *Msx1*$^{nlacZ/nlacZ}$ mutant embryo immunostained with the monoclonal antibody 4A6 and counterstained with H&E. This specimen displays a developed subcommissural organ (sco) and posterior commissure (pc), but the organ is not immunoreactive to 4A6, with the exception of some isolated

cells. **B:** Detail of the zone squared in panel A showing few immunoreactive subcommissural organ ependymal cells (arrows). **C:** Detail of a region similar to that squared in panel A of a consecutive section immunostained with anti-GAP43 showing the immunoreactive fibers of the posterior commissure (pc) over the subcommissural organ (sco). **D:** Detail of the region squared in panel A showing numerous pyknotic nuclei in the periaqueductal region. The calibration bar in panel D applies to panel A (180 µm); B (15 µm); C (40 µm); and D (30 µm).

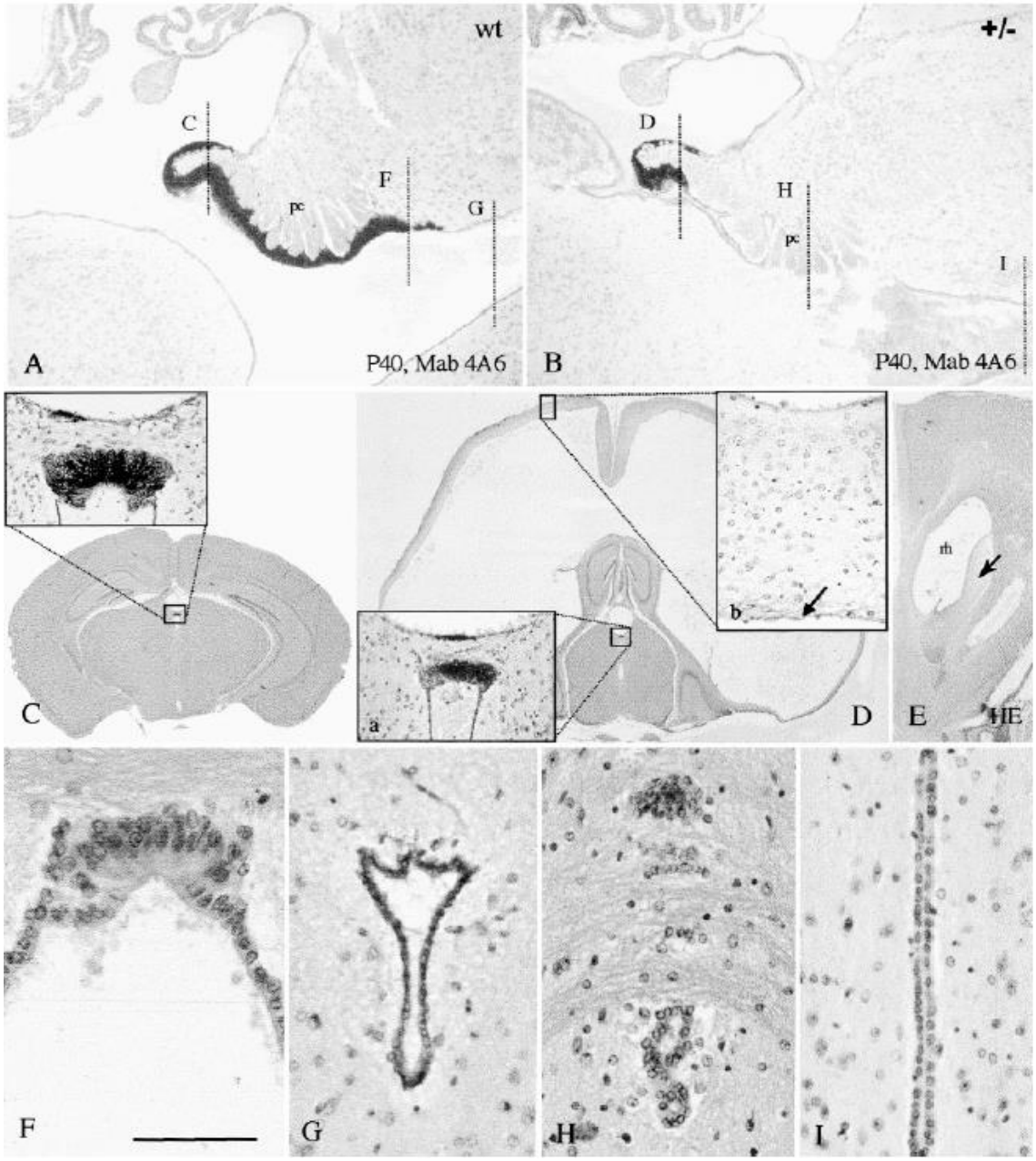

Fig. 6. A, B: Sagittal sections through the diencephalic dorsal midline of P40 wild-type and heterozygous *Msx1*$^{1/nlacZ}$ mutants, respectively, immunostained with monoclonal antibody 4A6 that selectively binds the secretory glycoproteins of the subcommissural

organ and counterstained with H&E. Note that in mutants the immunopositive secretory organ is highly reduced although the posterior commissure (pc) is present. The levels of the transverse sections are indicated in panels C–I. **C, D:** Panoramic survey of transverse sections through the brain of P40 wild-type and heterozygous *Msx1*$^{1/nlacZ}$ mutants, respectively, immunostained with monoclonal antibody 4A6 at the levels indicated in panels A and B (same magnification). The rostral region of the subcommissural organ is shown in detail in the inset in panel C and in panel D inset a. In mutants the immunoreactive organ is reduced to about 50% as compared to wild-type. Note the acute hydrocephalus of the lateral ventricles (lv) in mutants, the thinning of the cortex, and the absence of ependyma (inset b, arrow). **E:** Transverse section through the enlarged rostral horn (rh) of the lateral ventricle of a P40 heterozygous mutant showing subventricular cavitations and edema (arrow). **F, G:** Transverse sections through the levels indicated in panel A showing the immunoreactive caudal subcommissural organ and the open rostral aqueduct of wild-type mouse. **H, I:** Transverse sections through the levels indicated in panel B. Note disorganization of the caudal subcommissural organ and the rostral aqueduct with ependymal digitations and/or rosettes, some showing immunoreactive cells among the fibers of the posterior commissure (pc). The aqueduct is collapsed and no lumen is visible. The calibration bar in panel F applies to panel A and B (250 μm); C and D (2,200 μm); E (800 μm); F–I (60 μm); D (20 μm); and to insets (120 μm).